

Synchrony dual-optic accommodating intraocular lens

Part 1: Optical and biomechanical principles and design considerations

Stephen D. McLeod, MD, Luis G. Vargas, MD, Val Portney, PhD, Albert Ting, PhD

PURPOSE: To describe a dual-optic accommodating intraocular lens (IOL) based on theoretical considerations.

SETTING: University and independent research group.

METHODS: Ray-tracing analysis using optical modeling software (ZEMAX™, Focus Software Inc., Tucson, Ariz) in a theoretical model eye was used to analyze lens configurations to optimize the accommodative and magnification effects of axial lens displacement. Finite-element modelling using a commercially available PC-based software package (COSMOS DesignSTAR) was applied to design the biomechanical parameters of the inter-optic articulations and optics.

RESULTS: Ray-tracing analysis indicated that a dual-optic design with a high plus-powered front optic coupled to a minus posterior optic produced greater change in conjugation power of the eye compared to a single-optic intraocular lens and that magnification effects were unlikely to account for improved near vision. Finite-element modelling indicated that the 2 optics can be linked by spring-loaded haptics that allow anterior and posterior axial displacement of the front optic in response to changes in ciliary body tone and capsular tension.

CONCLUSION: A dual-optic design linked by spring haptics increases the accommodative effect of axial optic displacement with minimal magnification effect and has promise for improving the performance of accommodative intraocular lenses.

J Cataract Refract Surg 2007; 33:37–46 © 2007 ASCRS and ESCRS

Inexorable loss of accommodative amplitudes accompanies maturity. This presbyopic change has been attributed to various causes that include changes in the geometric relationships of the lens and the surrounding zonular and ciliary body structures based on progressive circumferential enlargement of the crystalline lens^{1–3} and changes in the elastic properties of the lens substance and capsule.^{4,5} Although reduced ciliary body function has been implicated in presbyopia, studies of aging rhesus monkeys confirm a robust ciliary body response to pharmacologic stimulation.^{5,6} In addition, magnetic resonance imaging studies of humans confirm that ciliary muscle contraction persists into the seventh decade.⁷

If presbyopia can be attributed to crystalline lens change despite persistent ciliary body function, replacement of the lens with a device that responds to ciliary body tone might restore accommodative function.

Contemporary accommodating intraocular lens (IOL) designs attempt to exploit the optical effect of anterior lens displacement that produces myopic shift and thus improve near vision; early clinical evaluation confirmed some degree of accommodative effect that is proportional to the measured optic displacement.^{8,9}

However, ray-tracing analysis indicates that the degree of accommodative effect is related not only to the degree of IOL displacement but also to the power of the displaced lens. A simple and rough approximation of the change in conjugation power of the system is provided by the following formula¹⁰:

$$\Delta D_c \approx (D_m/13)\Delta s$$

where ΔD_c is the change in the conjugation power of the eye, D_m is the dioptric power of the moving lens, and

Δs is the change in the lens position expressed in millimeters. Studies of changes in anterior chamber depth as an indicator of optic displacement suggest that axial movement is typically less than 1.0 mm.⁸ This is expected to produce variable and limited accommodative effect for the range of the IOL powers (+15.00 to +25.00 diopters [D]) most commonly implanted after cataract surgery.

If the degree of accommodative shift produced by forward axial displacement of a plus-power lens is proportional to the power of the lens, an accommodating IOL based on the principle of a high-plus-power moving lens coupled to a stationary optically compensatory minus lens should produce more consistent, higher amplitude accommodative shifts than current single-optic systems based on axial lens displacement.¹⁰

The arrangement of a plus-power lens coupled to a minus lens forms an optical system similar to a Galilean telescope configuration, with the important difference that this system creates the image at a finite and relatively short distance from the lenses (in this case, the retina) while a Galilean telescopic system includes a plus lens coupled to a minus eyepiece located within the prime focus of the plus lens to create a near-collimated beam the eye can then bring to focus with minimum accommodative effort.^{11,12}

The relationship between the design of a dual-optic accommodating IOL and telescope optics has implications for the potential role of magnification in the function of the IOL. A primary concern is that magnification leading to significant image-size disparity (aniseikonia) will preclude monocular implantation if the other eye remains phakic or is corrected with a single-optic IOL. Moreover, magnification might confound the interpretation of near-vision functional testing because improved performance compared to that of single-optic designs might be attributed to a magnification effect rather than a true change in the conjugation power of the eye.

The purpose of this study was to use optical and finite element modeling in the development and evaluation of

a dual-optic accommodating IOL, with attention to the implications of the potential magnification effects in such a system. A system of spring haptics joining the 2 optics was also designed using finite element modeling, intended to translate changes in ciliary body tone to axial displacement and thus optical power change.

MATERIALS AND METHODS

Optical Design: Accommodative and Magnification Effects

Given that a major limitation to the change in conjugation power induced by anterior lens displacement is the power of the lens, it was necessary to first quantify theoretically the effect of axial displacement of a typical accommodating IOL in the human eye and compare it with the effect of an alternative optical arrangement in which the power of the system is divided into a high-plus-power anterior-moving optic coupled to a static minus-power posterior optic. As described previously,¹⁰ ray-tracing analysis software (Zemax, Focus Software Inc.) using a theoretical model eye was used to analyze the expected optical effect of 1.0 mm axial movement of a single lens located at the plane of the posterior capsule. Assumptions used in constructing the model¹⁰ are shown in Table 1. Conjugation power change was calculated as change in refraction at the spectacle plane with vertex distance to the posterior spectacle surface of 12.0 mm and modeled over a range of theoretical IOL powers from +15.00 to +30.00 D. For comparison, the model was then used to calculate conjugation power change induced by anterior lens axial displacement of 1.0 mm for a dual-optic system with a 32.00 D anterior optic and a 0.5 mm posterior compensatory minus lens with power varied to produce a system ranging from +15.00 to +30.00 D.

The degree of image magnification produced on the retina by a dual-optic system was compared with that of a single-optic system with the lens 4.0 mm and 5.0 mm posterior to the posterior surface of the cornea in model eyes with 3 axial lengths: short (22.20 mm), medium (23.25 mm), and long (25.50 mm).

As described by Langenbucher et al.,¹³ any optical system can be considered a combination of refracting surfaces and interspaces between the surfaces. The angles at which a given ray meets and exits a refracting surface (ie, refraction), as well as the deviation from the optical axis that occurs during the passage of the ray through the interspace (translation), can be described as a linear coordinate transformation and specified in matrix form.^{14,15}

Table 1. Constants used in generating the theoretical model eye.¹⁰

Parameter	Value
Cornea index of refraction	1.3771
Aqueous index of refraction	1.3374
Lens index of refraction	1.43
Vitreous index of refraction	1.336
Cornea aspheric anterior vertex radius (mm)	7.8
Cornea aspheric posterior vertex radius (mm)	6.5
Cornea thickness (mm)	0.55
Anterior chamber depth (mm)	3.05
Second nodal point, posterior to corneal apex	7.51
Axial length (mm)	23.86

Accepted for publication September 4, 2006.

From the Department of Ophthalmology, University of California San Francisco (McLeod), San Francisco, Visiogen Inc. (Vargas, Ting), Irvine, and a private consultant (Portney), Tustin, California, USA.

Supported in part by unrestricted grants from That Man May See, San Francisco, California, and Research to Prevent Blindness, New York, New York, USA

Drs. McLeod, Vargas, Portney, and Ting have a financial interest in Visiogen Inc. and in the intraocular lens described.

Corresponding author: Stephen D. McLeod, MD, University of California San Francisco, Department of Ophthalmology, 10 Koret Way, K-304, San Francisco, California 94143, USA. E-mail: mcleods@vision.ucsf.edu.

The corresponding matrix of the optical system is called a power matrix:

$$S = \begin{pmatrix} a & b \\ c & d \end{pmatrix} \quad (1)$$

This power matrix is generated by specifying the refraction and translation matrices of all elements of the optical system and then multiplying them together in reverse order.

$$P = \begin{pmatrix} 1 & -R \\ 0 & 1 \end{pmatrix}, \text{refraction matrix of the surface with refractive power } R$$

$$T = \begin{pmatrix} 1 & 0 \\ t/n' & 1 \end{pmatrix}, \text{translation matrix of interspace (} t \text{) and medium refractive index (} n' \text{)}$$

The system power matrix now can be defined as

$$S = P_k \times T_{k-1} \cdots P_2 \times T_1 \times P_1 \quad (2)$$

This analysis used a reduced eye model¹⁶ in which the refractive powers of the anterior and posterior corneal surfaces were combined so the corneal power could be defined by a single surface (Appendix A).

This power matrix was applied to both the dual-optic IOL and single-optic IOL. Telescopic optical systems such as this manifest the greatest degree of magnification when the optics are most widely separated. Therefore, to model the scenario associated with the greatest degree of magnification in a dual-optic IOL, the lenses were set at the maximum separation for which the system is designed; that is, 1.5 mm. This is expected to produce about 4.00 D of object vergence (250 mm distance between the corneal vergence and object location). Table 2 shows the eye model and IOL parameters used for the evaluation.

The eye and dual-optic parameters are then converted to the parameters defining the refraction and translating matrices (Table 1, Appendix B). The power matrix of the system (equation 1) can then be constructed according to equation 2 and the locations of the system cardinal points determined. Table 2 in Appendix B lists the definitions of the cardinal points in power matrix terms as well as the focal length and image-object magnification as their derivatives.

Biomechanical Design

A review of the literature suggested the following biomechanical constraints within which an accommodating IOL must function: The typical diameter of the crystalline lens is approximately 9.5 mm, with a thickness of approximately 4.5 mm. After extracapsular cataract extraction, the capsular bag is estimated to be 10.5 mm in diameter.¹⁷ The force generated by the ciliary body, even in the presbyopic eye, is estimated to be 1 gram force (~10 mN).¹⁸

In the proposed model, to respond to ciliary body action, energy is stored and released in the lens system. A lens complex was designed with optics linked by articulations so that at rest outside the capsular bag, the optics are widely separated. When implanted in the capsular bag, centrifugal bag forces generated by zonular tension should compress the optics axially, reducing the interoptic separation and thus generating strain energy in the interoptic articulations. With accommodative effort, the zonules relax,

Table 2. Eye and IOL parameters used to model the retinal image magnification occurring in short, medium, and long eyes for 4.00 D of object vergence.

Parameter/Value	Comment
Axial length (mm)	
22.20	Short eye
23.25	Medium eye
25.50	Long eye
R ₁	
43.25	K-reading
t ₁ (ACD)	
4	Dual optic,
5	Single optic
r ₂	
5.963	Anterior lens front surface radius of dual optic
6.0	Front surface radius of single optic
t ₂	
1.3	Anterior lens thickness or single optic thickness
r ₃	
-5.963	Anterior lens back surface radius of dual optic
-5.4	Back surface radius of single optic (short eye)
-7.5	Back surface radius of single optic (medium eye)
-26.6	Back surface radius of single optic (long eye)
t ₃	
1.5	Anterior to posterior lens separation in dual optic
r ₄	
-7.25	Posterior lens front surface radius of dual optic
t ₄	
0.535	Posterior lens thickness in dual optic (short eye)
0.525	Posterior lens thickness in dual optic (medium eye)
0.375	Posterior lens thickness in dual optic (long eye)
r ₅	
-7.81	Posterior lens back surface radius of dual optic (short eye)
-13.343	Posterior lens back surface radius of dual optic (medium eye)
-24.082	Posterior lens back surface radius of dual optic (long eye)

ACD = anterior chamber depth

releasing the tension on the capsular bag, allowing release of the strain energy and forward movement of the anterior optic.

In the unaccommodated (far vision) position, the optics should be pulled together by the capsular bag. In the

accommodated (near vision) position, the lenses should move apart under the spring force of the haptics.

More specifically, in the unaccommodated state (distance focus), the ciliary body force is assumed to be near zero and the compressive force of the zonule and capsule structures is great enough to overcome the spring force of the lens complex so that the 2 optics are compressed. With accommodative effort (near focus), the compressive force of the zonule and capsule complex is counteracted or relieved by ciliary body force (assumed to be at its maximum, approximately 10 mN), allowing the zonules to move centripetally and releasing the spring haptics of the lens complex. While the posterior capsule and vitreous face provide stability for the posterior optic, the capsular bag release of the spring haptic allows forward movement of the front optic to an accommodated state. The system is therefore in varying states of force balance; however, accommodation occurs with the change in displacement of the apparatus under muscle force contraction that reduces the restoring force of the zonules and capsule to the point that the spring force of the haptics can produce anterior lens displacement.

Finite element modeling was applied to design the parameters of the interoptic articulations and optics using a commercially available PC-based software package (COSMOS DesignSTAR, Structural Research and Analysis Corp.). The following 2 material properties were entered into the model: (1) elastic modulus in tension; (2) Poisson's ratio, for a nearly incompressible, rubber-like material.

The entire lens was modeled with 10-node, solid tetrahedral elements. Element size was automatically varied to accurately represent the stress gradients in areas where stress concentration might occur. The posterior surface of the back lens was rigidly constrained in all directions. A unit displacement load was applied to the anterior surface of the front lens directed along the optic axis toward the back lens. Linear and nonlinear static analyses were performed. The resisting force under the applied load, stresses in the entire lens, and deformation of each node were calculated. The theoretical response of the IOL to applied loads was varied across numerous iterations by altering the thickness, length, and angles of the haptics in relation to the optic.

RESULTS

Optical Design

Ray-tracing analysis of the various scenarios modeled consistently demonstrated that anterior displacement of an exaggerated plus-power optic coupled to a compensatory static minus lens produced greater change in object distance than identical displacement of a single-optic lens of similar composite power. Figure 1 shows the degree of accommodative change for 1.0 mm displacement of a dual-optic system with a 32.00 D anterior optic separated by 0.5 mm from the appropriately powered posterior minus lens in the resting state compared with 1.0 mm displacement of a single-optic IOL. As expected, the optical efficiency of the single-optic system met that of the dual-optic system as the power of the optic was increased.

The positions of the cardinal points and their derivatives, including image-object magnification, are presented for the dual-optic IOL in Table 3 and for the single-optic IOL in Table 4. The values of the cardinal points are

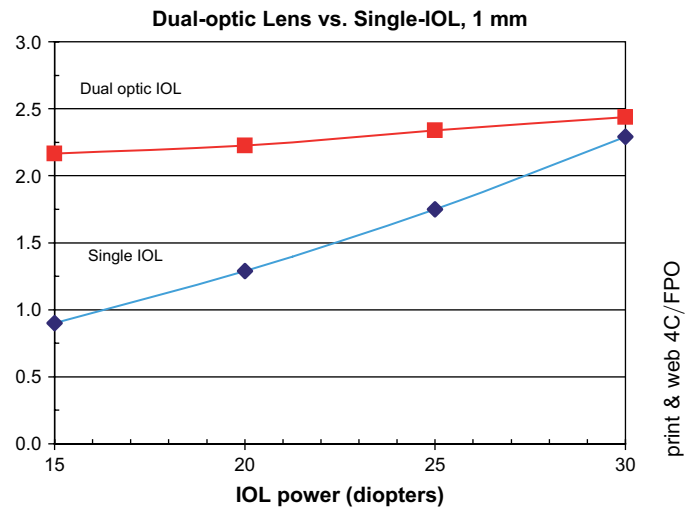


Figure 1. Accommodative change calculated by ray-tracing analysis for 1.0 mm movement of a single-optic IOL for powers ranging from 15.00 to 30.00 D compared to a dual-optic IOL with a 32.00 D anterior-moving lens coupled to a variably powered static posterior lens. Constants used in the model eye are shown in Table 1. The curves show that at high lens powers, the accommodative effect of axial displacement of a single lens is similar to that of the dual-optic design; however, although the accommodative effect is preserved at low powers in a dual-optic system, that effect is greatly reduced at low powers for a single-optic IOL.

provided in terms of the eye's anatomical characteristics (ie, distance from the corneal vertex). Negative values refer to the location to the left from the vertex and positive values, to the right from the vertex.

The optical effect of the construction of the dual-optic IOL is that of shifting the cardinal point toward the object from the locations of the equivalent cardinal points of a single-optic IOL for the same eye configuration. This results in a slight increase in focal lengths and magnification.

One can express the relative increase in magnification by application of the following formula

$$\Delta M = \frac{M_{\text{dual-optic}} - M_{\text{single-optic}}}{M_{\text{single-optic}}}$$

This leads to the calculation of a relative increase in magnification by 1.00% for the short eye, 2.16% for the medium eye, and up to 2.50% for the long eye.

Biomechanical Design

Based on the parameters entered into the finite element model described in Materials and Methods, a dual-optic single-piece IOL connected by 4 spring haptics was designed (Figure 2).

Assuming some degree of elasticity in the peripheral capsular bag, as the anterior optic moves in the anterior and posterior directions it was assumed that there would

Table 3. Retinal image magnification calculated in short, medium, and long eyes with 4.00 D of vergence for a dual-optic IOL: cardinal points and their derivatives.

Parameter	Short Eye	Medium Eye	Long Eye
Dual-optic eye system power matrix	$\begin{pmatrix} 0.8888 & -69.636 \\ 0.0052 & 0.71669 \end{pmatrix}$	$\begin{pmatrix} 0.9185 & -65.568 \\ 0.0052 & 0.71711 \end{pmatrix}$	$\begin{pmatrix} 0.9697 & -58.129 \\ 0.0051 & 0.72465 \end{pmatrix}$
First focal point (F ₁)	-12.76	-14.008	-16.682
Second focal point (F ₂)	21.085	21.937	23.83
First principal point (P ₁)	1.597	1.244	0.521
Second principal point (P' ₂)	1.900	1.561	0.847
First nodal point (N ₁)	6.422	6.368	6.301
Second nodal point (N' ₂)	6.725	6.685	6.627
First focal length (EFL ₁)	14.36	15.25	17.203
Second focal length (EFL ₂)	19.185	20.376	22.984
Image distance from second principal point	20.30	21.69	24.65
Image vergence (D)	65.811	61.60	54.19
Object distance from first principal point	-261.47	-251.87	-253.97
Image vergence (D)	3.824	3.97	3.94
Magnification (M _{dual-optic})	-0.05811	-0.06445	-0.07266

be some change in the volume of aqueous captured between the optics in the capsular bag. Therefore, to facilitate fluid exchange, protuberances on the anterior optic were added that served to tent the capsulorhexis edge up from the front surface of the optic, preserving an avenue for aqueous flow. To control the optical power of the system at rest when under capsular bag tension, the optics were pulled together; spacers were placed between the optics to control the minimum optic separation.

The design advanced to fabrication, constructed using silicone with a refractive index of 1.43 with a length of 9.5 mm and width of 9.8 mm. When compressed, the total lens thickness was 2.2 mm, and the haptics were designed to allow 1.5 mm of optic movement with relaxation of the capsular bag due to ciliary body contraction. Fatigue testing was performed on three prototypes in order to demonstrate sustained spring force through repeated cycles. The dual-lens system was mounted in a water bath and a piston

Table 4. Retinal image magnification calculated in short, medium, and long eyes with 4.00 D of vergence for a single-optic IOL: cardinal points and their derivatives.

Parameters	Short Eye	Medium Eye	Long Eye
Single-optic eye system power matrix	$\begin{pmatrix} 0.857 & -70.9297 \\ 0.0046 & 0.78661 \end{pmatrix}$	$\begin{pmatrix} 0.8801 & -66.973 \\ 0.0046 & 0.78661 \end{pmatrix}$	$\begin{pmatrix} 0.9227 & -59.668 \\ 0.0046 & 0.78661 \end{pmatrix}$
First focal point (F ₁)	-12.082	-13.14	-15.465
Second focal point (F ₂)	21.116	21.99	23.913
First principal point (P ₁)	2.017	1.791	1.295
Second principal point (P' ₂)	2.281	2.043	1.522
First nodal point (N ₁)	6.754	6.808	6.926
Second nodal point (N' ₂)	7.018	7.06	7.153
First focal length (EFL ₁)	14.098	14.93	16.76
Second focal length (EFL ₂)	18.836	19.95	22.39
Image distance from second principal point	19.92	21.21	23.98
Image vergence (D)	67.07	63.00	55.72
Object distance from first principal point	-259.12	-251.59	-253.14
Image vergence (D)	3.86	3.97	3.95
Magnification (M _{single-optic})	-0.05754	-0.06309	-0.0709

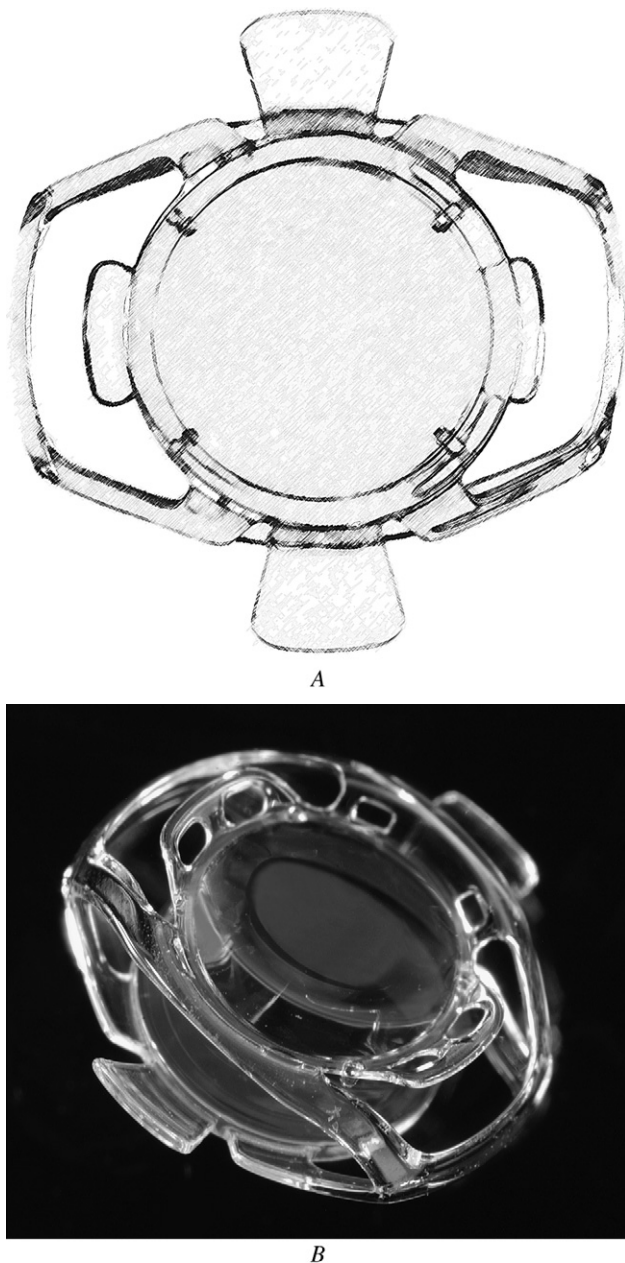


Figure 2. A: Schematic of the anterior surface of the Synchrony dual-optic accommodating IOL prototype that was fabricated and tested. The spring haptics are located at the 3 o'clock and 9 o'clock positions and stabilizing elements at the 12 o'clock and 6 o'clock positions. The entire complex measures 9.8 mm horizontally and 9.5 mm vertically. B: Photograph of the dual-optic accommodating IOL prototype viewed in three-quarter profile shows the high-plus-power moving anterior optic (*above*) coupled to the compensatory minus-power static posterior optic (*below*) by spring haptics. The structures elevated above the plane of the anterior optic are designed to tent the anterior capsule up from the anterior surface of the front optic, allowing aqueous exchange between the interlenticular space and the anterior chamber.

system used to apply near sinusoidal compression and release at 3 Hz, for greater than 250 000 cycles. The compression force was measured before and after cyclic fatigue testing; the posttest reduction in pretest compression force of all lenses at 3.6% was found to be within the error band of the measurement system.

DISCUSSION

The optical design we present consists of a dual-optic system with an exaggerated plus-power optic coupled to a compensatory minus-power static lens. Ray-tracing analysis showed the design may produce consistent and amplified accommodative amplitudes designs across a wide range of IOL powers compared to a single moving optic.¹⁰ This arrangement might be erroneously interpreted as similar to that of a telescopic design, but the spatial arrangement and relative lens powers produce minimum image magnification compared to focal shift. As such, this design is expected to greatly improve the predictability and range of accommodating IOLs and can be considered for monocular and binocular implantation.

Whereas we used commercially available ray-tracing software to model the optical effect of a dual-optic accommodative system, Langenbucher et al.¹³ used linear geometric matrix analysis based on the Gullstrand eye model to describe the properties of such a system. This alternative analysis confirmed a nearly constant accommodation amplitude in the range of 2.40 to 2.50 D per millimeter. Moreover, these investigators explored the effect of symmetric anterior translation and posterior translation of the anterior and posterior lenses, respectively, and determined that although this would reduce the accommodative effect compared to anterior movement of the anterior optic with a stationary posterior optic, the focus shift would still exceed that of comparable anterior displacement of a single-optic IOL in a similarly modeled eye.

A minimal magnification effect was observed in this analysis of a dual-optic accommodating IOL system. There are 2 effects to consider when magnification may be clinically significant: (1) the introduction of aniseikonia between the eyes if aphakia in 1 eye is corrected with a single-optic IOL and in the other with a dual-optic IOL; (2) the effect on the visual acuity when evaluating the accommodating ability of the dual-optic IOL. The normal tolerance for aniseikonia has been measured to be between 5% and 8% by different methods,¹⁹ and image-size disparity above this level is expected to prevent fusion leading to a bothersome binocular image and symptoms of aniseikonia.^{19–22} The results in this study demonstrate that the upper range of magnification disparity between an eye with single-optic IOL and another with the dual-optic IOL design is on the order of 2.5%. This is well below the level

at which symptoms resulting from aniseikonia would be expected to occur, is comparable to the image-size disparity established between aphakic contact lens and single-optic IOL correction, and is not expected to impact binocular visual function.

This analysis also allows us to consider whether simple magnification introduced by the dual-optic design rather than a true accommodative change in focal length might lead to improved near-vision test results compared with results with a single-optic IOL. To measurably enhance visual acuity based on magnification, the increase in image size should approach the height difference from 1 line to the next. In the case of the Early Treatment Diabetic Retinopathy Study chart, consecutive lines increase in height by a factor of 1.2589.^{23,24} Therefore, one might estimate that a magnification increase of 25% would be required to improve testing scores by 1 line. However, the upper range of magnification associated with the dual-optic design in this analysis was on the order of 2.5%. This degree of magnification is unlikely to contribute significantly to the performance of the IOL.

The dual-optic design incorporates connecting spring haptics that allow maximum articulation between capsule tension and the lens system, allowing more direct communication with ciliary body tone because in effect, the system is designed to fill the capsular bag and expand against both the anterior and posterior capsules. The effect this might have on capsular bag contraction, residual lens epithelial cell migration and capsular bag contraction is the subject of ongoing animal and clinical trials.²⁵

The potential effect of increasing capsular rigidity deserves further consideration. In the resting state, for zonular tension to be transmitted to the lens complex, the capsular bag must compress the system. This requires a degree of capsule contraction around the lens complex. Subsequent accommodative motion of the lens requires that ciliary body contraction and relaxation be transmitted directly to the lens via changes in zonular and capsular bag tension. Excessive capsule laxity or elasticity is expected to attenuate ciliary body and zonular movement; the effect is analogous to that of pulling an object with a loose elastic band rather than with a steel cable. Progressive capsule fibrosis and contraction will ultimately lead to system failure if the spring force of the system is overwhelmed.

Review of the literature suggested that the risk for interlenticular opacification was greatly reduced with double-optic designs using silicone,²⁶⁻³³ so this material was used in the fabrication of initial foldable prototypes. Werner et al.²⁵ examined the characteristics of capsule fibrosis after implantation of this dual-optic IOL in a rabbit model and compared the results with those of a single-piece plate-haptic silicone IOL. They report significantly reduced

degrees of opacification and capsule contraction in eyes with the dual-optic IOL than in control eyes. Clinical studies are necessary to confirm that the profound retardation of capsule fibrosis noted in the rabbit model extends to the clinical situation in humans.

In summary, we designed a dual-optic accommodating IOL that based on theoretical considerations is anticipated to produce a higher and more consistent degree of accommodative change compared to single-optic devices based on axial optic displacement. There was no significant magnification for either a single- or dual-lens system at any theoretical eye axial length studied, and magnification effects are therefore unlikely to contribute to the performance of this configuration of a dual-optic design. The clinical evaluation of this device is the subject of ongoing study.

REFERENCES

1. Koretz JF, Handelman GH. Modeling age-related accommodative loss in the human eye. *Math Model* 1986; 7:1003-1014
2. Schachar RA. Zonular function: a new hypothesis with clinical implications. *Ann Ophthalmol* 1994; 26:36-38
3. Gilmartin B. The aetiology of presbyopia: a summary of the role of lenticular and extralenticular structures. *Ophthalmic Physiol Opt* 1995; 15:431-437
4. Tamm E, Lütjen-Drecoll E, Jungkunz E, Rohen JW. Posterior attachment of ciliary muscle in young, accommodating old, presbyopic monkeys. *Invest Ophthalmol Vis Sci* 1991; 32:1678-1692
5. Croft MA, Kaufman PL, Crawford KS, et al. Accommodation dynamics in aging rhesus monkeys. *Am J Physiol* 1998; 275(6, pt 1):R1885-R1897
6. Poyer JF, Kaufman PL, Flügel C. Age does not affect contractile responses of the isolated rhesus monkey ciliary muscle to muscarinic agonists. *Curr Eye Res* 1993; 12:413-422
7. Strenk SA, Semmlow JL, Strenk LM, et al. Age-related changes in human ciliary muscle and lens: a magnetic resonance imaging study. *Invest Ophthalmol Vis Sci* 1999; 40:1162-1169
8. Langenbacher A, Seitz B, Huber S, et al. Theoretical and measured pseudophakic accommodation after implantation of a new accommodative posterior chamber intraocular lens. *Arch Ophthalmol* 2003; 121:1722-1727
9. Marchini G, Pedrotti E, Santori P, Tosi R. Ultrasound biomicroscopic changes during accommodation in eyes with accommodating intraocular lenses; pilot study and hypothesis for the mechanism of accommodation. *J Cataract Refract Surg* 2004; 30:2476-2482
10. McLeod SD, Portney V, Ting A. A dual optic accommodating foldable intraocular lens. *Br J Ophthalmol* 2003; 87:1083-1085
11. Kingslake R. *Lens Design Fundamentals*. New York, NY, Academic Press, 1978; 259-268
12. Smith WJ. *Modern Optical Engineering: the Design of Optical Systems*, 3rd ed. New York, NY, McGraw-Hill, 2000
13. Langenbacher A, Reese S, Jakob C, Seitz B. Pseudophakic accommodation with translation lenses—dual optic vs mono optic. *Ophthalmic Physiol Opt* 2004; 24:450-457
14. Rosenblum WM, Christensen JL. Optical matrix method: optometric applications. *Am J Optom Physiol Optics* 1974; 51:961-968
15. Keating MP. Lens effectivity in terms of dioptric power matrices. *Am J Optom Physiol Opt* 1981; 58:1154-1160
16. Atchison DA, Smith G. *Optics of the Human Eye*. Boston, MA, Butterworth Heinemann, 2000; 250-254

17. Assia EI, Apple DJ. Side-view analysis of the lens. Part I. The crystalline lens and the evacuated bag. *Arch Ophthalmol* 1992; 110:89–93
18. Fisher RF. The force of contraction of the human ciliary muscle during accommodation. *J Physiol (Lond)* 1977; 270:51–74
19. Crone RA, Leuridan OMA. Unilateral aphakia and tolerance of aniseikonia. *Ophthalmologica* 1975; 171:258–263
20. Schechter RJ. Elimination of aniseikonia in monocular aphakia with a contact lens-spectacle combination. *Surv Ophthalmol* 1978; 23: 57–61
21. Garcia M, González C, Pascual I, Fimia A. Magnification and visual acuity in highly myopic phakic eyes corrected with an anterior chamber intraocular lens versus by other methods. *J Cataract Refract Surg* 1996; 22:1416–1422
22. Rubin ML. Contemporary management of aniseikonia. *Surv Ophthalmol* 1997; 41:321–330
23. Bailey IL, Lovie JE. New design principles for visual acuity letter charts. *Am J Optom Physiol Opt* 1976; 53:740–745
24. Ferris FL III, Kassoff A, Bresnick GH, Bailey I. New visual acuity charts for clinical research. *Am J Ophthalmol* 1982; 94:92–96
25. Werner L, Pandey SK, Izak AM, et al. Capsular bag opacification after experimental implantation of a new accommodating intraocular lens in rabbit eyes. *J Cataract Refract Surg* 2004; 30:1114–1123
26. Gayton JL, Apple DJ, Peng O, et al. Interlenticular opacification: clinicopathological correlation of a complication of posterior chamber piggyback intraocular lenses. *J Cataract Refract Surg* 2000; 26: 330–336
27. Werner L, Shugar JK, Apple DJ, et al. Opacification of piggyback IOLs associated with an amorphous material attached to interlenticular surfaces. *J Cataract Refract Surg* 2000; 26:1612–1619
28. Eleftheriadis H, Marcantonio J, Duncan G, Liu C. Interlenticular opacification in piggyback AcrySof intraocular lenses: explanation technique and laboratory investigations. *Br J Ophthalmol* 2001; 85:830–836
29. Trivedi RH, Izak AM, Werner L, et al. Interlenticular opacification of piggyback intraocular lenses. *Int Ophthalmol Clin* 2001; 41:47–62
30. Gayton JL, Van der Karr M, Sanders V. Neodymium:YAG treatment of interlenticular opacification in a secondary piggyback case. *J Cataract Refract Surg* 2001; 27:1511–1513
31. Eleftheriadis H, Sciscio A, Ismail A, et al. Primary polypseudophakia for cataract surgery in hypermetropic eyes: refractive results and long term stability of the implants within the capsular bag. *Br J Ophthalmol* 2001; 85:1198–1202
32. Werner L, Apple DJ, Pandey SK, et al. Analysis of elements of interlenticular opacification. *Am J Ophthalmol* 2002; 133:320–326
33. Spencer TS, Mamalis N, Lane SS. Interlenticular opacification of piggyback acrylic intraocular lenses. *J Cataract Refract Surg* 2002; 28: 1287–1290

APPENDIX A

Power Matrix Modeling of Magnification in a Pseudophakic Human Eye: Cardinal Points (Cardinal Planes)

The locations of the principle planes (P_1 and P_2) and nodal planes (N_1 and N_2) are different if the refractive indices in the object space and image space are different. The corresponding cardinal points are defined by the intersection of the system optical axis with the corresponding planes. The distance between the principle plane and corresponding focal point determines the effective focal length. The nodal planes are characterized by the property such that the angle at which a ray enters the nodal plane matches the angle at which it exits the other nodal plane. This implies that the image position is maintained as the system is rotated around the second nodal point. For instance, the second nodal point in the eye system is close to the center of eye rotation, leading to insensitivity of the image location at the retina to small eye movements.

APPENDIX B

Paraxial Characteristics of a Pseudophakic Eye with a Dual-Optic Intraocular Lens

By convention, the locations of the cardinal points are defined in terms of the distances from the front surface (corneal vertex) in the object space and from the last surface (back surface vertex) in the image space. In case of the reduced eye model with the dual-optic in place, the first surface is the composite corneal refracting surface and the last surface is the back surface of the dual-optic posterior lens (Tables 1 and 2). The optical science definition is different from the locations measured anatomically, which is determined from the front vertex of the cornea or from the retinal surface. The optical science definition can be easily converted to the anatomical definition for known axial length L of the eye.

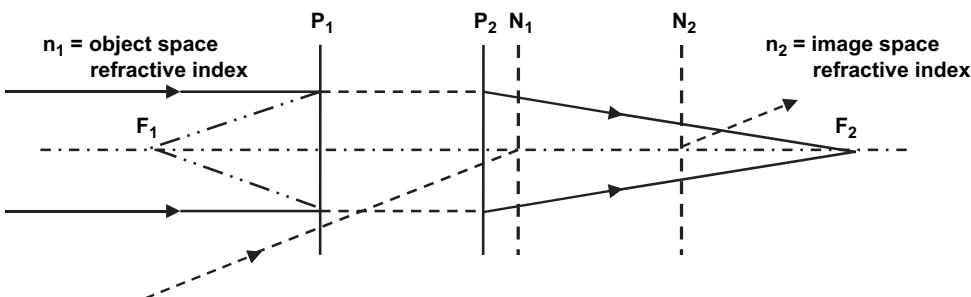


Figure A1. Power matrix modeling of magnification in a pseudophakic human eye: cardinal points (cardinal planes).

Table 1. Eye model parameters for the dual-optic IOL.

Matrix Parameter	Definition
First refraction surface = corneal surface K-reading	$R_1 = K = \frac{337.5}{r_1}$ <p>where K = K-reading and r_1 = corneal radius(*) t_1, n_a = aqueous refractive index (1.336)</p>
First interspace = anterior chamber depth	
Second refraction surface = power of front surface or conventional IOL or front surface of anterior lens of dual-optic IOL	$R_2 = \frac{1000 \times (n_a - n')}{r_2}$ <p>where n_a = refractive index of anterior lens material, n' = aqueous refractive index (1.336), and r_2 = surface radius t_2, n_a = refractive index of anterior IOL material</p>
Second interspace = anterior lens thickness or conventional lens thickness	
Third refraction surface = power of back surface of conventional IOL or back surface of anterior lens of the dual-optic IOL	$R_3 = \frac{-1000 \times (n_a - n')}{r_3}$ <p>where n_a = refractive index of anterior lens material, n' = aqueous refractive index (1.336), and r_3 = surface radius t_2, n' = aqueous refractive index (1.336)</p>
Third interspace = separation between anterior and posterior lenses in the dual-optic IOL	
Fourth refraction surface = power of front surface of posterior lens of the dual-optic IOL	$R_4 = \frac{-1000 \times (n_p - n')}{r_4}$ <p>where n_p = refractive index of posterior lens material, n' = aqueous refractive index (1.336), and r_4 = surface radius t_4, n_p = refractive index of posterior lens material</p>
Fourth interspace = posterior lens thickness	
Fifth refraction surface = power of back surface of posterior lens of the dual-optic IOL	$R_5 = \frac{-1000 \times (n_p - n')}{r_5}$ <p>where n_p = refractive index of anterior lens material, n' = aqueous refractive index (1.336), and r_5 = surface radius</p>

*Radii are in millimeters with conventional optical science sign nomenclature. The light travels from left to right, and the sign is positive if it is along the ray direction and negative otherwise.

Table 2. Application of the power matrix to a model eye: definition of cardinal points and their derivatives

Cardinal Point or Its Derivative	Formula from the Power Matrix Defined by Optical Science	Anatomical or Eye-Related Definitions
Lens T = lens system total length	$T = \sum_{i=1}^5 t_i$ distance between corneal and last refraction surface	Anterior segment length (ASL)
	$J = L - T$ where L = eye axial length	Posterior segment length
First (object) focal point	$F_1 = 1000 \times n \times \frac{a}{b}$ where n = object space refractive index = 1 (air)	Eye focal length
Second (image) focal point	$F_2 = 1000 \times n' \times \frac{-d}{b}$ where n' = image space refractive index = 1.336 (aqueous)	—
First (object) principal point	$H_1 = 1000 \times n \times \frac{a-1}{b}$ where n = object space refractive index = 1 (air)	First (object) principal point
Second (image) principal point	$H_2 = 1000 \times n' \times \frac{1-a}{b}$ where n' = image space refractive index = 1.336 (aqueous)	Second (image) principal point measured from cornea: $H'_2 = T - H_2$
First (object) nodal point	$N_1 = 1000 \times \frac{a \times n - n'}{b}$ where n = object space refractive index = 1 (air) and n' = image space refractive index = 1.336 (aqueous)	First (object) nodal point
Second (image) nodal point	$N_2 = 1000 \times \frac{n - d \times n'}{b}$ where n = object space refractive index = 1 (air) and n' = image space refractive index = 1.336 (aqueous)	Second (image) nodal point measured from cornea: $N'_2 = T - N_2$
First (object) focal length = distance between first principal point and first focal point	$EFL_1 = 1000 \times n \times \frac{-1}{b}$	Eye focal length
Second (image) focal length = distance between second principal point and second focal point	$EFL_2 = 1000 \times n' \times \frac{1}{b}$	—
Image distance = distance between second principal point and image plan	$I = L - T + H_2 = L - H'_2$	—
Image vergence (D)	$V' = 1000 \times n' \times \frac{1}{I}$ where I = image distance	—
Magnification = ratio of image size to object size	$M = 1 + \frac{b}{V'}$	Magnification
Object vergence (D)	$V = -b - V'$	Object vergence